JCB Article

Annexin 11 is required for midbody formation and completion of the terminal phase of cytokinesis

Alejandra Tomas, Clare Futter, and Stephen E. Moss

Division of Cell Biology, Institute of Ophthalmology, London EC1V 9EL, England, UK

Annexins are Ca^{2+}-binding, membrane-fusogenic proteins with diverse but poorly understood functions. Here, we show that during cell cycle progression annexin 11 translocates from the nucleus to the spindle poles in metaphase and to the spindle midzone in anaphase. Annexin 11 is recruited to the midbody in late telophase, where it forms part of the detergent-resistant matrix that also contains CHO1. To investigate the significance of these observations, we used RNA interference to deplete cells of annexin 11. A combination of confocal and video time-lapse microscopy revealed that cells lacking annexin 11 fail to establish a functional midbody. Instead, daughter cells remain connected by intercellular bridges that contain bundled microtubules and cytoplasmic organelles but exclude normal midbody components such as MKLP1 and Aurora B. Annexin 11–depleted cells failed to complete cytokinesis and died by apoptosis. These findings demonstrate an essential role for annexin 11 in the terminal phase of cytokinesis.

Introduction

Annexin 11 is one of a large family of calcium-dependent phospholipid-binding proteins with roles in calcium signaling, apoptosis, and vesicle trafficking (for review see Gerke and Moss, 2002). Annexins appear to be present in all eukaryotic phyla except yeasts, and most mammalian cell types express a subset of family members. Of the dozen vertebrate family members, annexin 11 is believed to be the most evolutionarily ancient (Fernandez et al., 1996; Morgan et al., 1998). Like all annexins, it contains multiple tandem repeats of a 70–amino acid domain in which the Ca^{2+}-binding sites are located, but in common only with annexin 7, it has a long NH_2 terminus rich in glycine, proline, and tyrosine residues (Tokumitsu et al., 1992; Towle and Treadwell, 1992). Annexin 11 is ubiquitously expressed and has been identified in the nucleus in most cultured cell lines studied (Mizutani et al., 1992; Farnaes and Ditzel, 2003; Tomas and Moss, 2003). Despite the absence of a recognizable nuclear localization signal in the NH_2 terminus, mutagenesis experiments have identified this domain as being required for targeting of annexin 11 to the nucleus (Mizutani et al., 1995).

The NH_2-terminal domain of annexin 11 has also been shown to contain the binding sites for at least two intracellular polypeptide ligands, namely calcyclin (S100A6) and the apoptosis-linked protein ALG-2 (Tokumitsu et al., 1993; Satoh et al., 2002). In both cases, the interaction between annexin 11 and its ligand has been shown in in vitro experiments to be Ca^{2+} dependent, but neither the purpose of the interaction nor indeed the function of either of the participating proteins is known. The differential expression of calcyclin during the cell cycle (Calabretta et al., 1986) and evidence that annexin 11 may have a role both in mitosis (Mizutani et al., 1992) and in nuclear envelope dynamics during prophase (Tomas and Moss, 2003) prompted us to examine more closely the subcellular localization of annexin 11 during the different stages of cell division. We show here that from late mitosis through to cytokinesis, annexin 11 colocalizes with established components of the central spindle and midbody, such as CHO1 and the Aurora B kinase. Furthermore, in experiments using siRNA we show that cells depleted of annexin 11 do not present a midbody matrix at the middle of the central spindle, and subsequently undergo abortive cell separation in which daughter cells remain connected by bridgelike cytoplasmic structures and ultimately die by apoptosis. These results demonstrate an essential function for annexin 11 in the last phase of cytokinesis.

Results

The localization of annexin 11 is regulated during the cell cycle

To find out if the subcellular localization of annexin 11 is regulated during cell division, we used confocal immunoflu-

The online version of this article includes supplemental material.

Address correspondence to S.E. Moss, Division of Cell Biology, Institute of Ophthalmology, 11-43 Bath St., London EC1V 9EL, England, UK. Tel.: 020 7608 6973. Fax: 020 7608 4034. email: s.moss@ucl.ac.uk

Key words: calcium; mitosis; telophase; cell cycle; kinesin

Abbreviations used in this paper: BFA, brefeldin A; RNAi, RNA interference.

The Journal of Cell Biology

orescence microscopy to track annexin 11 through the late stages of the cell cycle in conjunction with α-tubulin in A431 cells (Fig. 1 A). From the nucleus of interphase cells (unpublished data), annexin 11 partially relocates to the degenerating nuclear envelope during prophase, which is consistent with our previous findings (Tomas and Moss, 2003). In metaphase, annexin 11 is distributed throughout the cell but with greatest intensity at the mitotic half-spindles, also consistent with a recent paper describing colocalization of annexin 11 and α-tubulin in COS-7 cells (Farnaes and Ditzel, 2003). As the chromosomes segregate during anaphase, annexin 11 concentrates along the central spindle, eventually becoming focused at the midzone and ultimately in the midbody at cytokinesis. The specificity of the antisera used in these experiments was demonstrated by pre-adsorption of the primary antibody with affinity-purified annexin 11 protein before immunostaining (Fig. 1 B), and the localization of annexin 11 at the midbody was confirmed by costaining with antisera to the cytokinesis-associated protein kinase Aurora B (Terada et al., 1998; Fig. 1 C).

To exclude the possibility that these observations were a peculiarity of A431 cells, we immunostained HeLa and HEp2 cells in cytokinesis (Fig. 2 A). These cells also revealed annexin 11 at the midbody as well as in the regenerating nuclear envelope in HEp2. In higher resolution images of A431, HeLa, and HEp2 cells, annexin 11 immunoreactivity at the midbody had the appearance of two parallel discs positioned at the center of and perpendicular to the central spindle, which persisted as part of the midbody remnant that connects two daughter cells after furrow ingression is completed (Piel et al., 2001; Fig. 2, B–D). Although the annexin 11 discs appear to "cap" the facing ends of the microtubule bundles at these extreme late stage midbodies, the staining probably defines the lateral borders of the midbody matrix.

To explore the relationship between annexin 11 and midbody formation in greater detail, A431 cells were blocked at prometaphase with nocodazole, and then released into brefeldin A (BFA). In *Caenorhabditis elegans*, BFA has been shown to disrupt the terminal phase of cytokinesis, most likely by inhibiting the targeted secretion of membrane vesicles to the late cleavage furrow (Skop et al., 2001). Consistent with these observations, A431 cells furrowed normally in the presence of BFA (Fig. 2 E), but then became binucleate after the failure of the terminal phase of cytokinesis (Fig. 2 F). In the presence of BFA, the staining intensity for annexin 11 at the midbody was increased and concentrated in a disc concentric to the actomyosin contraction ring and spanning its internal diameter (Fig. 2 G). Therefore, the localization of annexin 11 to the midbody proved to be BFA insensitive, suggesting that annexin 11 is not a component of the membrane vesicles targeted to the midbody but a constituent of the midbody matrix. This idea was further supported in BFA-treated cells costained for annexin 11 and the Golgi marker GM130, in which the Golgi-derived vesicles, thought to be the source of membrane targeted to the cleavage furrow during the terminal phase of cytokinesis (Hill et al., 2000; Lecuit and Wieschaus, 2000), did not costain for annexin 11 (Fig. S1, available at http://www.jcb.org/cgi/content/full/jcb.200311054/DC1).

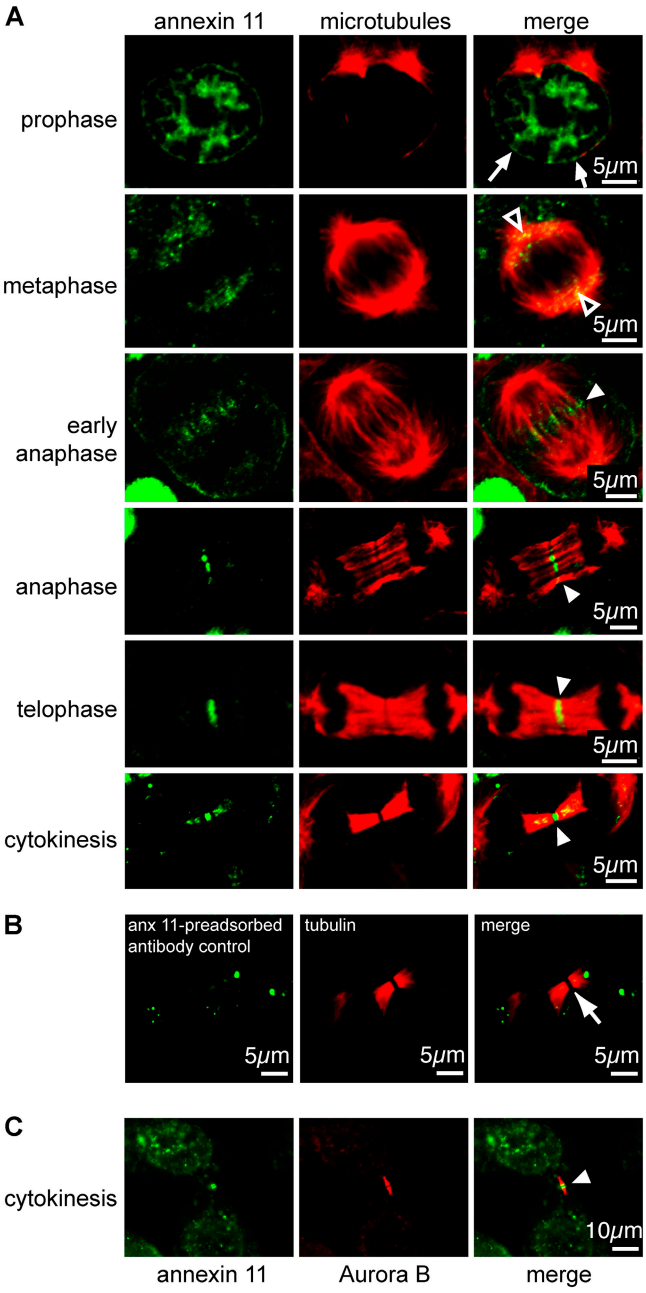

Figure 1. **Immunolocalization of annexin 11 at the different stages of the cell cycle.** (A) A431 cells were fixed at different stages of cell cycle progression and stained for α-tubulin and annexin 11. Annexin 11 is predominantly localized to the nucleoplasm and nuclear envelope during NEB (prophase, arrows), with enrichment toward the centrosomes and the spindle in metaphase (open arrowheads). In anaphase and telophase, annexin 11 concentrates in the midzone region (closed arrowheads) with intense staining at the midbody during cytokinesis. (B) Control experiment showing A431 cells at cytokinesis immunostained for α-tubulin and annexin 11, but with the latter antibody pre-adsorbed with affinity-purified GST-annexin 11. The arrow in the merged image points to the absence of annexin 11 immunoreactivity at the midbody. (C) A431 cells at cytokinesis were fixed and immunostained as in B for annexin 11 and the kinase Aurora B. The merged image (right) shows colocalization of annexin 11 and Aurora B at the midbody (arrowhead).

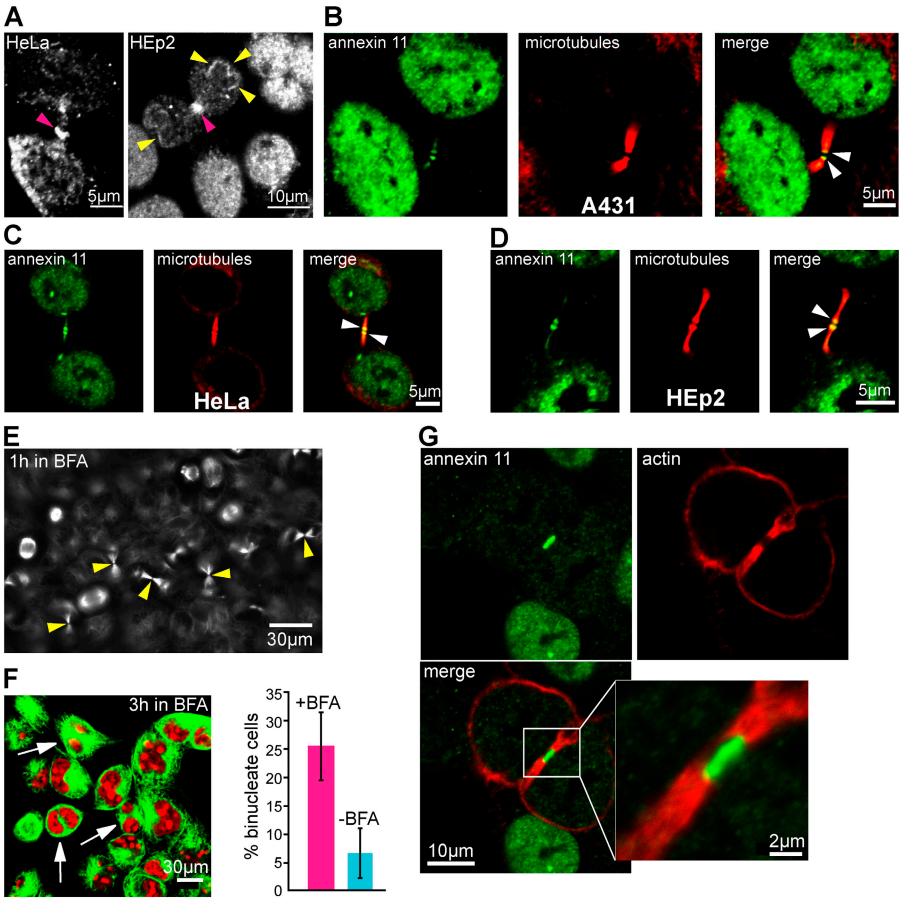

Figure 2. **Annexin 11 is a component of the midbody in different cell lines.** (A) HeLa and HEp2 cells were fixed in cytokinesis and stained for annexin 11. The pink arrowheads indicate annexin 11 at the midbody, whereas the yellow arrowheads highlight the localization of annexin 11 to the reforming nuclear envelope in the daughter HEp2 cells. A431 (B), HeLa (C), and HEp2 (D) cells were fixed in cytokinesis and stained for annexin 11 and α-tubulin. In B, C, and D, annexin 11 is organized as two parallel discs at either side of the midbody remnant (arrowheads), perpendicular to the central spindle. (E and F) A431 cells were blocked in prometaphase with nocodazole, followed by treatment with BFA for 1–3 h. Cells were subsequently fixed and stained for α-tubulin and DNA (with propidium iodide; F). After 1 h of BFA treatment (E), ∼20% of the cells were in late anaphase or telophase (yellow arrowheads). After 3 h of treatment (F), numerous binucleate cells were detected among the recently divided cells (white arrows). For quantitative evaluation of the effects of BFA, A431 cells were synchronized with thymidine overnight, incubated for 6 h in nocodazole, and then released for 3 h in the presence or absence of BFA. Cells were fixed and stained for α-tubulin and DNA with DAPI. Binucleate and total cell counts were performed. Results are the average of five counts from two different Petri dishes. (G) Synchronized and BFA-treated A431 cells were fixed and stained for annexin 11 and for F-actin (with TRITC-phalloidin). The image shows a cell in cytokinesis and a zoom-in across the cleavage furrow. Annexin 11 is located in the midbody at the center of the actomyosin constriction ring formed at the furrow.

Annexin 11 associates with midbody components during cytokinesis

The staining pattern of annexin 11 from anaphase to cytokinesis bears striking similarities to that reported for the mitotic kinesin-like protein CHO1, an alternatively spliced product of the *MKLP1* gene with essential roles in the maintenance of the microtubule bundles at the central spindle and in the organization of the midbody matrix (Matuliene and Kuriyama, 2002). To further investigate a possible relationship between these two proteins, we examined their localization in A431 cells at various times in the cell cycle (Fig. 3 A). Although annexin 11 and CHO1 are predominantly nuclear in interphase and metaphase cells, there is no tight colocalization at this time. However, from anaphase through to cytokinesis, and at the midbody, there is marked colocalization of annexin 11 and CHO1. Both proteins are also highly enriched in isolated midbodies (Fig. 3 B). This finding is consistent with previous reports for CHO1 (Sellitto and Kuriyama, 1988) and indicates that the association of annexin 11 with this structure is stable.

CHO1 has previously been shown to physically interact with microtubules (Kuriyama et al., 1994), F-actin (Kuriyama et al., 2002), and the small G-protein Arf3 (Boman et al., 1999). We performed pull-down experiments to investigate whether tubulin or CHO1 also associate with annexin 11. A431 cells were either collected immediately after prometaphase block or further treated with BFA and collected at cytokinesis, the latter resulting in an enrichment of annexin 11 at the midbody. Under these cell lysis conditions, and regardless of whether cells were extracted at prometaphase or cytokinesis, >90% of annexin 11 appeared in the soluble fraction (Fig. 3 C). Immunoprecipitation of annexin 11 from the postnuclear supernatants resulted in the sequestration of ∼70% of the solubilized fraction. Western blotting revealed the presence of CHO1 in immunoprecipitates of annexin 11 specifically during late mitosis and cytokinesis, whereas tubulin was present in both prometaphase- and cytokinesis-derived immune complexes (Fig. 3 D). A mock immunoprecipitation using control goat IgG in place of anti–annexin 11 failed to yield CHO1 upon Western blotting though tubulin was detected, suggesting that although the presence of CHO1 in the annexin 11 immunoprecipitates reflects a specific interaction, the tubulin may be at least to some extent a contaminant. The control blot (Fig. 3 D) confirms approximately equal band intensities for annexin 11 in the immunoprecipitates. Western blotting of whole cell lysates prepared from cells synchronized at prometaphase and cytokinesis revealed bands of equal intensities for CHO1, tubulin, and annexin 11 (Fig. 3 E), confirming that the presence of CHO1 in the annexin

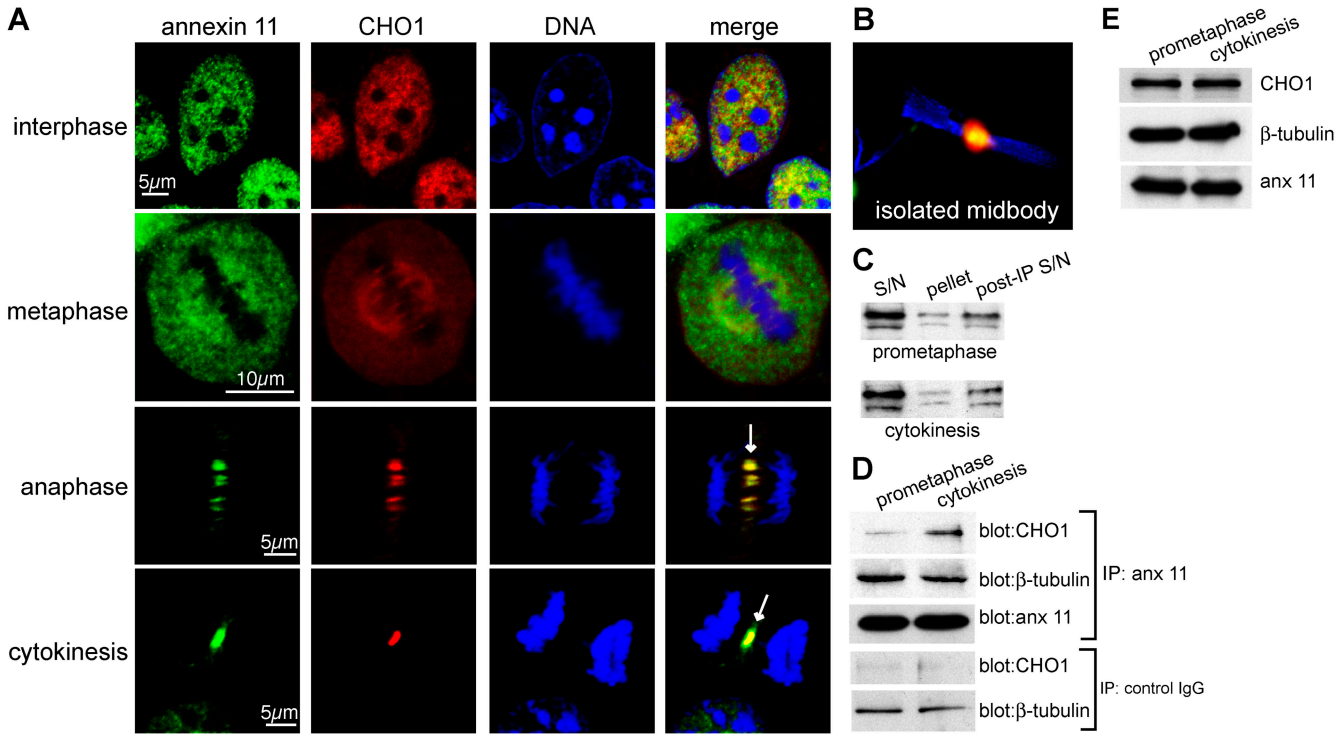

Figure 3. **Annexin 11 colocalizes and interacts with CHO1 at cytokinesis.** (A) A431 cells were synchronized in mitosis and fixed and stained for annexin 11 and CHO1. DNA was labeled with propidium iodide. Cells in interphase through to cytokinesis are depicted. Both annexin 11 and CHO1 are located mainly inside the nucleus during interphase and are excluded from the nucleoli. During metaphase, CHO1 relocates along the spindle while annexin 11 is dispersed throughout the cell, though with some enrichment at the spindle. From anaphase onwards, both proteins extensively colocalize, first at the central spindle, then at the midzone, and ultimately in the midbody during cytokinesis (arrows). (B) A431 cells were synchronized and collected in cytokinesis. Midbodies were isolated as described in Materials and methods, adsorbed onto polylysine-coated coverslips, and stained for annexin 11 (green), α-tubulin (blue), and CHO1 (red). CHO1 and annexin 11 intensely colocalize at the center of the isolated midbody. (C) A431 cells were synchronized at prometaphase and cytokinesis and solubilized in lysis buffer (see Materials and methods for details). The lysate was centrifuged and the post-nuclear supernatant (S/N) and pellet were resolved by SDS-PAGE and probed for annexin 11 by immunoblotting. After immunoprecipitation, the post IP supernatant was also immunoblotted to evaluate the degree of immunodepletion. (D) A431 cells were synchronized at prometaphase, and either harvested immediately or incubated in BFA for 1 h and collected in cytokinesis. Cells were lysed, and annexin 11 was immunoprecipitated and resolved by SDS-PAGE. After Western blotting, filters were probed for CHO1, β-tubulin, and annexin 11 (to confirm equal loadings). The two bottom panels show blots for CHO1 and β-tubulin after mock immunoprecipitation using a control goat IgG. (E) A431 cells were synchronized at prometaphase or cytokinesis as in C, and whole cell lysates were resolved by SDS-PAGE followed by Western blotting for CHO1, β-tubulin, and annexin 11.

11 immunoprecipitates at cytokinesis does not simply reflect increased cellular levels of CHO1 at this point in the cell cycle. Together, these results show that annexin 11 indeed interacts (directly or indirectly) with CHO1 during cytokinesis, and support the idea that annexin 11 and CHO1 are constituents of a midbody multiprotein complex.

Annexin 11 knockdown inhibits completion of cytokinesis and leads to apoptosis

To investigate the role of annexin 11 in cytokinesis, we used RNA interference (RNAi) to depress the level of annexin 11 in A431 and HeLa cells. Incubation with a 21-base pair RNA duplex corresponding to nucleotides gACggCTTACggCAAggAT of annexin 11 led to a time-dependent decrease in the levels of annexin 11 protein and mRNA (Fig. 4, A and B), although the kinetics of annexin 11 depletion appeared more rapid in A431 cells. In HeLa cells, after two rounds of transfection over 6 d, annexin 11 was barely detectable by Western blotting or RT-PCR, whereas closely related molecules such as annexin 1 and annexin 5 were unchanged. Immunofluorescence analysis of HeLa cells after 5 d in annexin 11 siRNA revealed the absence of detectable annexin 11 staining in the nucleus, with residual punctate annexin 11 staining in the cytoplasm (Fig. 4 C). These results demonstrate the efficacy and specificity of siRNA-mediated suppression of annexin 11 expression in this experimental system.

To investigate the annexin 11 null phenotype in greater detail, we cultured HeLa and A431 cells for 2 d in annexin 11 siRNA and analyzed them by immunofluorescence. HeLa cells undergoing cytokinesis appeared to furrow normally but lacked the dense material located in the middle of the central spindle corresponding to the midbody matrix (Fig. 5 A). The absence of the midbody matrix is clear when contrasted against control cells in which the immunostaining for α-tubulin is completely missing from the equator of the central spindle due to the inability of the antibody to access the microtubules through the matrix (Matuliene and Kuriyama, 2002; Fig. 5 B). Confocal microscopy of fixed A431 cells immunostained for α-tubulin revealed that de-

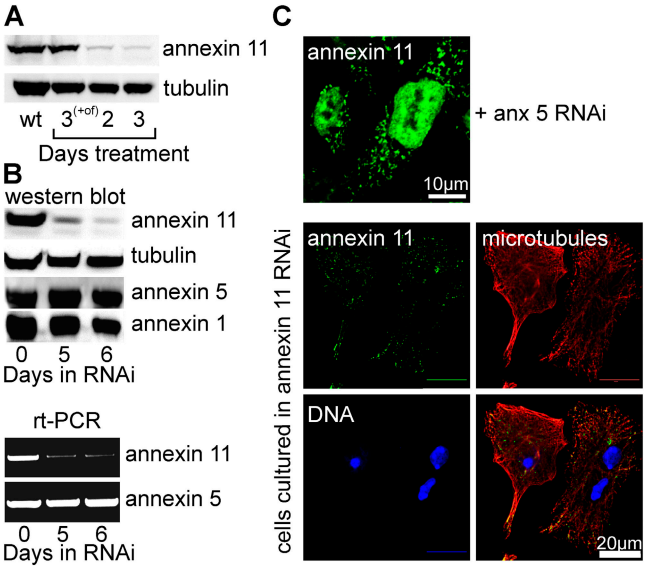

Figure 4. **Depletion of annexin 11 using siRNA.** (A) A431 cells were treated with siRNA for annexin 11, with oligofectamine alone (+of) or with no additives (wt) for the periods indicated. Whole cell lysates were resolved by SDS-PAGE and immunoblotted for annexin 11 and α-tubulin. Note that the level of annexin 11 drops after 2 d of siRNA treatment. (B) HeLa cells were cultured in 24-well plates and treated with siRNA. Cells were lysed after 5 and 6 d of treatment and analyzed by Western blotting and RT-PCR. Note that the levels of annexin 11 cDNA and protein are significantly decreased by day five, whereas the levels of annexins 1 and 5 remain unchanged. (C) HeLa cells were treated for 5 d with siRNA specific for annexin 11 or 5 (control), and then fixed and stained for annexin 11, α-tubulin, and DNA (with propidium iodide). Note that the green fluorescence corresponding to annexin 11 is still present in cells treated with annexin 5 siRNA, but is significantly diminished in cells treated with annexin 11 siRNA.

pletion of annexin 11 similarly leads to failure to establish a midbody matrix and accumulation of microtubule bundles (Fig. 5 C), where the matrix is normally located in control cells (Fig. 5 D). Electron microscopy of annexin 11–depleted A431 cells confirms that midbodies fail to form and shows that microtubule bundles and endoplasmic reticulum are distributed throughout the area where the midbody would normally form (Fig. 6). These results show that in distinct cell types annexin 11 is required for formation of the midbody matrix.

To examine the effects of annexin 11 depletion on the distribution of established midbody proteins, we immunostained A431 cells undergoing abortive cytokinesis for MKLP1 and Aurora B kinase. As expected, in control cells MKLP1 localized predominantly to the midbody in cells at cytokinesis (Fig. S2, available at http://www.jcb.org/cgi/content/full/jcb.200311054/DC1). However, in cells depleted of annexin 11 that fail to form a midbody, MKLP1 remained concentrated in the daughter nuclei, which is consistent with its localization in normal interphase cells (Chen et al., 2002). The apparent failure of MKLP1 to exit the nucleus is consistent with an essential role for annexin 11 in the recruitment of midbody proteins and midbody assembly, though it is also possible that MKLP1 targets correctly in late telophase and then regresses to the nucleus when cytokinesis fails. In contrast, Aurora B was concentrated at the lateral borders of the midbody in control A431 cells at cytokinesis, but was expressed along the full length of the extended intracellular cytoplasmic bridge in annexin 11–depleted cells (Fig. S2). Although Aurora B has not yet been ascribed a role at the midbody, the modest effect of annexin 11 depletion on Aurora B localization is consistent with annexin 11 having a function in cytokinesis that lies temporally downstream of the known role of Aurora B in spindle assembly and chromosome segregation.

Phase-contrast time-lapse imaging revealed marked differences between control and annexin 11 siRNA-treated A431 cells undergoing cytokinesis (Fig. 7, A and B; and Videos 1 and 2, available at http://www.jcb.org/cgi/content/full/jcb.200311054/DC1). Depletion of annexin 11 resulted in a highly abnormal cellular morphology characterized by cell bodies connected by long cytoplasmic bridgelike extensions. The images of live cells entering cytokinesis show that although furrowing progresses normally in annexin 11–depleted cells, abscission does not occur (Fig. 7 B). Instead, the daughter cells become separated by increasingly thin cytoplasmic extensions, a process that is accompanied by rounding up of the optically refractive cell bodies, eventual detachment from the surface of the coverslip, and cell death. To extend these observations to a large cell population, we performed flow cytometry on A431 cells at various stages of culture in annexin 11 siRNA (Fig. 7 C). By measuring forward scatter, we observed an increase in cell length at days two and three, corresponding to the peak period of abortive cytokinesis, after which cell/particle size diminished as the cells died and fragmented.

To test whether or not the cell death that we observed in the RNAi experiments was apoptotic, we performed a PARP immunoblot on cells after annexin 11 depletion. This experiment revealed the presence of cleaved PARP in annexin 11 siRNA-treated A431 cells (Fig. 7 D), which was indicative of caspase activation and apoptosis (Scovassi and Poirier, 1999). In HeLa and A431 cells cultured in siRNA for annexin 11, stained with propidium iodide, and analyzed by flow cytometry, we observed a decrease in 2n and 4n peaks through day three to five after transfection, together with a concomitant increase in the sub-2n nuclear pool, a further diagnostic feature of apoptosis (Fig. 7, E–G). Cells cultured in siRNA for annexin 5 showed no such changes. By day four of annexin 11 siRNA treatment in A431 cells, and by day six in HeLa cells, we observed >70% apoptotic cell death (Fig. 7 F) as judged by quantification of the flow cytometry data, by which time cells also exhibited the typical morphological blebbing associated with apoptosis (not depicted).

Discussion

We have shown here that annexin 11, a predominantly nuclear protein during interphase, exhibits a tightly regulated pattern of localization during the latter stages of the cell cycle from prophase to cytokinesis. This pattern is typical of several midbody proteins, and we show that annexin 11 tracks especially closely with the mitotic kinesin-like protein CHO1 (Matuliene and Kuriyama, 2002). Because

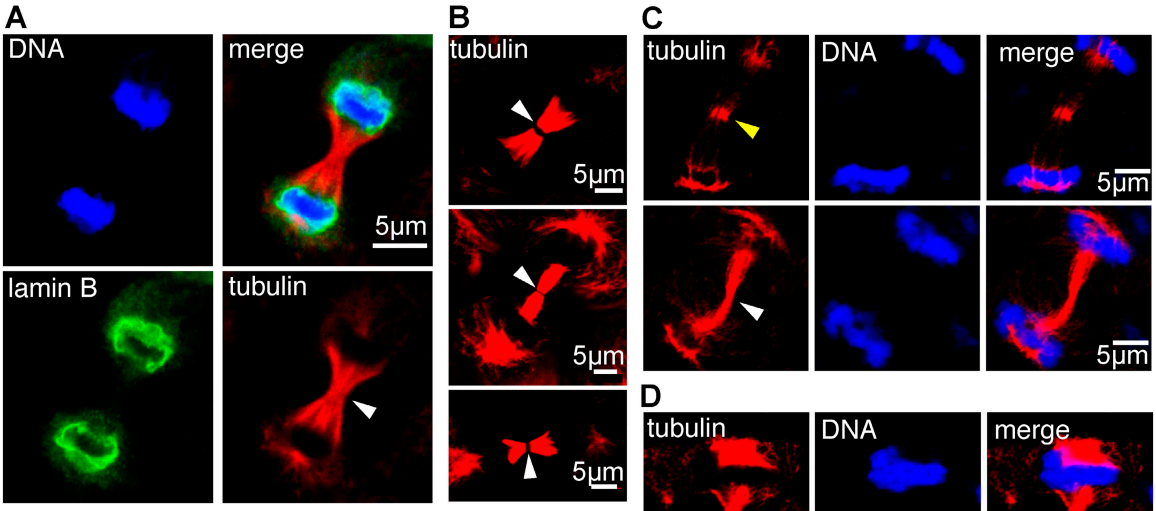

Figure 5. **Annexin 11 is required for midbody matrix formation.** (A) HeLa cells treated with annexin 11 siRNA for 2 d were fixed and stained for lamin B and α-tubulin. DNA was labeled using propidium iodide. The merged image shows an intact microtubular bridge between the two daughter nuclei, but with no midbody matrix (arrowhead). (B) HeLa cells were synchronized, fixed in cytokinesis, and stained for α-tubulin. In three representative cells, the midbody matrix (arrowheads) is clearly visible as a narrow band from which α-tubulin staining is excluded. (C) A431 cells were treated with annexin 11 siRNA and fixed and stained after 2 d for α-tubulin and DNA as in A. Two examples show an abnormal enrichment of α-tubulin at the midbody center (yellow arrowhead) and failure to establish a midbody matrix (white arrowhead). (D) Control A431 cells fixed and immunostained at cytokinesis reveal exclusion of α-tubulin staining at the midbody matrix, as observed in B for HeLa cells.

CHO1 has been reported to engage in interactions with microtubules, F-actin, and Arf3, we investigated the possibility that annexin 11 may also form part of what appears to be a midbody multiprotein complex. Coimmunoprecipitation experiments revealed that annexin 11 and CHO1 not only become enriched at the midbody but also physically associate, either directly or indirectly, from late mitosis through to cytokinesis. This association appears to be specific for this stage of the cell cycle, as it is not present in nocodazole-treated cells blocked at prometaphase. Like

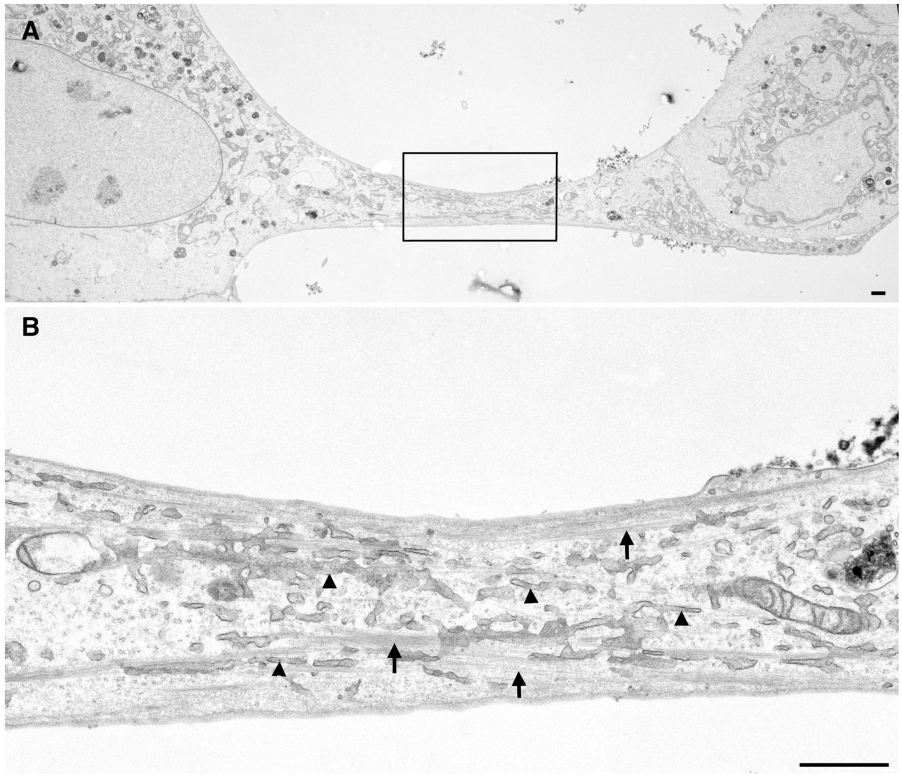

Figure 6. **Electron microscopy shows a complete absence of midbody formation in annexin 11–depleted cells.** A431 cells were treated with annexin 11 siRNA for 3 d, and were then fixed and processed for electron microscopy. Low magnification view (A) shows a cytoplasmic bridge between adjacent cell bodies. The area indicated is enlarged in B to show the absence of a midbody and the distribution of microtubule bundles (arrows) and endoplasmic reticulum (arrowheads) throughout the area where the midbody would normally form. Bars, 1 μm.

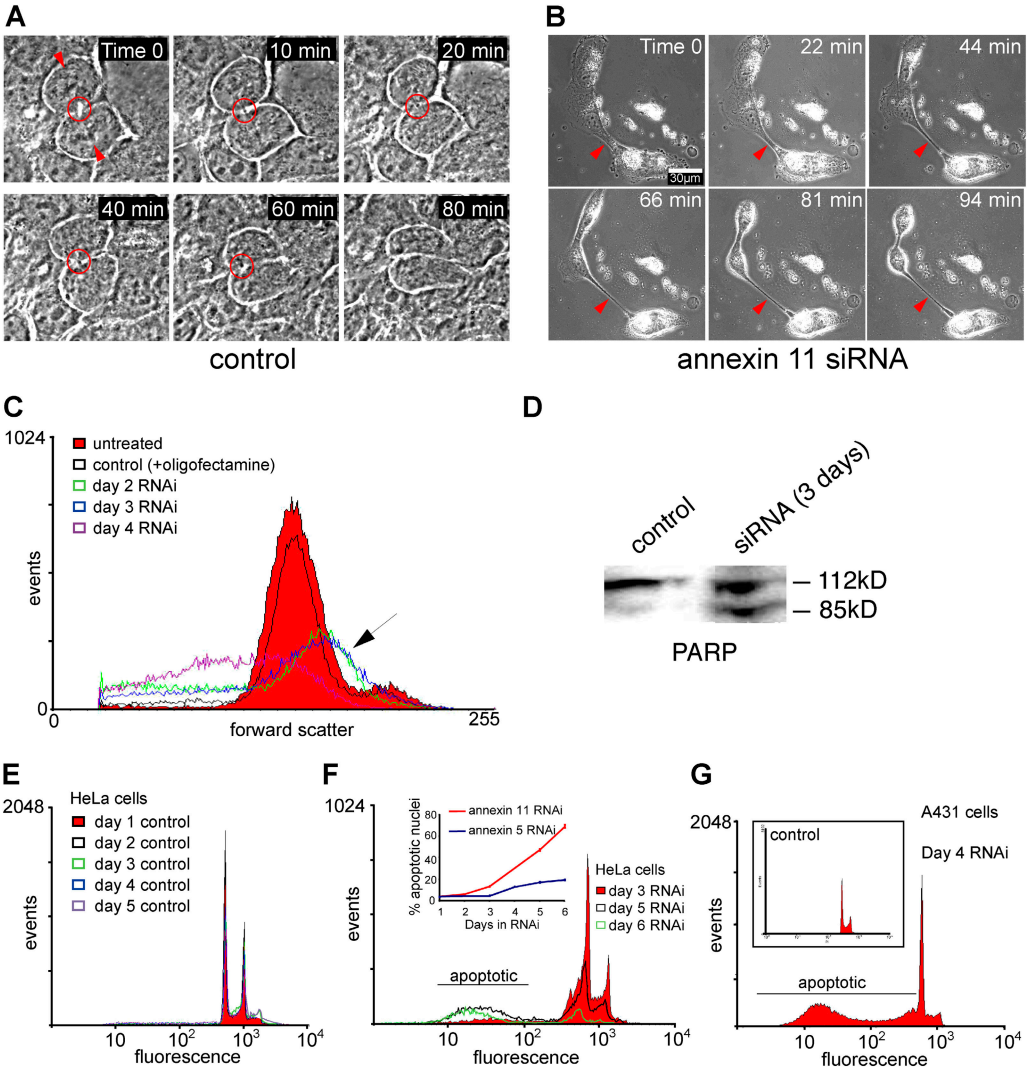

Figure 7. **Cytokinesis failure and apoptosis in cells treated with annexin 11 siRNA.** (A) Control A431 cells undergoing cytokinesis were examined by video time-lapse microscopy (see Video 1). The two dividing cells are marked by red arrowheads at time 0, and the midbody is at the center of the red circle. By 80 min, cytokinesis was complete and the midbody was no longer visible. (B) A431 cells were treated for 2 d in annexin 11 siRNA, and video time-lapse microscopy was performed on cells attempting cytokinesis (see Video 2). The cells remain connected by a cytoplasmic bridge that becomes increasingly narrow but is never resolved (red arrowheads). After 94 min, the cells had shrunk and rounded up. They subsequently detached and drifted out of the field of view (not depicted). (C) A431 cells were treated with annexin 11 siRNA and examined for changes in cell size/shape by flow cytometry. The arrow indicates an increase in forward scatter (indicating increased cell length) at days two and three, which subsequently diminishes by day four. (D) A431 cells were treated for 3 d with annexin 11 siRNA or with oligofectamine alone as a control, and total cell lysates were resolved by SDS-PAGE and immunoblotted for PARP. Note the 85-kD band corresponding to the cleavage product of PARP in annexin 11–depleted cells. (E and F) HeLa cells were treated with annexin 5 siRNA (control, E) or annexin 11 siRNA (F) for indicated periods and analyzed by flow cytometry. Note that the sub-2n (apoptotic) peak increases substantially during days five and six for annexin 11 siRNA-treated cells compared with the control. The inset graph (F) provides numerical representation of the FACS® data. (G) A431 cells were treated with annexin 11 siRNA for 4 d and examined by flow cytometry. The inset shows cells treated with oligofectamine alone as a control. Note the sub-2n (apoptotic) peak present in annexin 11–depleted cells but absent in the control.

CHO1, annexin 11 also associates with tubulin, though the annexin 11–tubulin interaction was evident at both prometaphase and cytokinesis.

In a recent study it was noted that CHO1 is the only protein so far identified as a component of the detergent-resistant midbody matrix (Matuliene and Kuriyama, 2002). Our demonstration here that annexin 11 also remains tightly associated with the midbody after biochemical isolation confirms annexin 11 as the second characterized protein of this matrix. Moreover, depletion of annexin 11 by RNAi in A431 and HeLa cells leads to the absence of a detectable midbody matrix at cytokinesis, showing that annexin 11 is required for the formation of this matrix in at least two different human cell lines. The only other protein known to be required for the formation of the midbody matrix is CHO1. Thus, overexpression of a mutant form of CHO1 that is unable to concentrate in the midbody or a significant reduction in the level of endogenous CHO1 by RNAi treatment both resulted in cells furrowing normally but lacking a midbody matrix during telophase and cytokinesis (Matuliene and

Kuriyama, 2002). However, complete depletion of CHO1 by RNAi also caused disorganization of the central spindle microtubule bundles, indicating a dual function for CHO1 in cytokinesis, both in the formation of a midbody matrix and in the maintenance of the central spindle organization. This last phenotype was not observed in annexin 11–depleted cells, implying that the function of annexin 11 in cytokinesis is linked exclusively to the formation of a midbody matrix and completion of the terminal phase of cytokinesis. Significantly, failure to form a midbody as a result of annexin 11 depletion led to mislocalization of CHO1. Taken with previous published work (Matuliene and Kuriyama, 2002), this finding suggests that annexin 11 and CHO1 are both indispensable for midbody formation, supporting the idea that the two proteins are in some way functionally linked.

In cells treated with siRNA specific for annexin 11, the last stage of cytokinesis is highly impaired, with daughter cells entering interphase while still connected by abnormal cytoplasmic bridges that they are unable to resolve, and eventually undergoing cell death by apoptosis. Although in most reported examples of failed cytokinesis, furrow regression and cell binucleation occur before cell death, there are a few instances of abortive cytokinesis in which daughter cells remain connected by bridgelike cytoplasmic structures. These instances include overexpression of a mutant form of CHO1 (Matuliene and Kuriyama, 2002); siRNA-mediated depletion of centriolin (Gromley et al., 2003); overexpression of the Rho inhibitory domain of Nir2, a RhoA-binding protein that associates with the small GTPase in the cleavage furrow (Litvak et al., 2002); cells transfected with a mutant form of the type III intermediate filament protein GFAP lacking its Rho-kinase phosphorylation sites (Yasui et al., 1998); and the blockage of phosphatidylethanolamine translocation at the cleavage furrow (Emoto and Umeda, 2000), which inhibits disassembly of the actomyosin constriction ring. These studies collectively define a subset of midbody proteins that, like annexin 11, are likely to be functionally coordinated to execute the final stages of cytokinesis.

The discovery of an essential role for annexin 11 in cell division is unexpected when considered in the broader context of annexin biology. Although annexins are now firmly implicated in various cellular activities, including endocytosis, calcium signaling, and apoptosis, no member of this protein family has been demonstrated to function in the cell cycle. The membrane binding and vesicle fusogenic properties that define annexins in biochemical terms could provide clues as to the possible role of annexin 11 in the last stage of cytokinesis. Before cells can be completely separated in a process known as abscission, the actomyosin constriction ring at the cleavage furrow has to be disassembled and the central spindle must separate. During this series of events, it is likely that the plasma membrane must be tightly attached to the midbody microtubules for abscission to be successfully completed. CHO1 has previously been suggested to be responsible for this connection (Kuriyama et al., 2002), but there is no evidence that this kinesin is able to bind to the cell membrane. The role of annexin 11 could be to facilitate this interaction. Alternatively, annexin 11 could be involved in the vesicle fusion process that mediates the insertion of new membrane at the cleavage furrow, which is widely established as a key requirement for completion of cytokinesis (Straight and Field, 2000), or it may have a role in the rearrangement of membrane phospholipids at the cleavage furrow, which is known to be crucial for the disassembly of the actomyosin constriction ring (Emoto and Umeda, 2000). In mammalian cells the origin of the membrane or vesicular material that is inserted at the cleavage furrow has not been formally identified. In *Drosophila melanogaster*, it has been reported that Golgi-derived membrane is required for furrow formation during cellularization (Sisson et al., 2000), and Golgi-associated proteins such as Arf1 (Altan-Bonnet et al., 2003) and syntaxin 5 (Xu et al., 2002) have been shown to have roles in cytokinesis. Here, we found no evidence of annexin 11 association with Golgi-derived vesicles, suggesting that annexin 11 is more likely to be involved in membrane dynamics at the cleavage furrow than in vesicle transport to this site.

In this context, it is interesting to note that annexin 11 is not expressed in invertebrates, and is therefore absent in the two experimental models most used for the study of cytokinesis, namely *D. melanogaster* and *C. elegans*. It is possible that unrelated annexins present in these organisms fill this function, or it may be that the role of annexin 11 in cytokinesis is performed by other proteins in simpler eukaryotes.

Materials and methods

Cell lines and culture conditions

Human A431, HeLa, and HEp2 cells were grown in DME (GIBCO BRL) supplemented with 10% (vol/vol) FCS, 100 U/ml penicillin, 100 μg/ml streptomycin, and 292 μg/ml L-glutamine at 37°C in 5% CO_2 humidified incubators. Cells were kept subconfluent, and the medium was changed every 2 to 3 d. For microscopy, cells were plated onto sterilized coverslips or grown in 35-mm glass bottom microwell dishes (MatTek).

Antibodies

Antibodies used for immunofluorescence were L-19 goat polyclonal anti–human annexin 11 (Santa Cruz Biotechnology, Inc.), mouse monoclonal anti–mouse annexin 11 (BD Biosciences), mouse monoclonal anti–chicken α-tubulin (Zymed Laboratories), rabbit polyclonal anti–human α-tubulin (gift of K. Matter, Institute of Ophthalmology, University College London, London, UK), E18 rabbit polyclonal anti–chicken CHO1 (gift of R. Kuriyama, University of Minnesota, Minneapolis, MN; Kuriyama et al., 2002), mouse monoclonal anti–rat Aim-1 (BD Biosciences), N-19 rabbit polyclonal anti-MKLP1 (Santa Cruz Biotechnology, Inc.), E-15 goat polyclonal anti-ARK-2 (Santa Cruz Biotechnology, Inc.), and M-20 goat polyclonal anti–mouse lamin B (Santa Cruz Biotechnology, Inc.). Secondary antibodies were donkey anti-goat-Alexa Fluor 488 (Molecular Probes), goat anti–mouse-Alexa Fluor 488 (Molecular Probes), donkey anti–mouse-Alexa Fluor 488 (Molecular Probes), donkey anti–rabbit-Cy5, donkey anti–mouse-Cy5, and donkey anti–mouse-TRITC. Antibodies used for Western blotting were as for CHO1, L-19 goat polyclonal anti–human annexin 11 (Santa Cruz Biotechnology, Inc.), sheep polyclonal anti–chicken annexin 11 (raised against full-length recombinant chicken annexin 11), mouse monoclonal anti–chicken α-tubulin (Zymed Laboratories), mouse monoclonal anti–β-tubulin (Sigma-Aldrich), and rabbit polyclonal anti–human PARP (Santa Cruz Biotechnology, Inc.). Antisera to annexins 1 and 5 have been described previously (Hawkins et al., 1999).

Cell synchronization and isolation of midbodies

Cells were grown to 50% confluence and incubated in medium containing 4 mM thymidine (Sigma-Aldrich) overnight to achieve S phase block. Dishes were extensively washed in PBS and cultured for a further 6 h in medium containing 0.07 μg/ml nocodazole (Sigma-Aldrich) for growth arrest at prometaphase. Cells were extensively washed and allowed to recover in normal medium for 30–60 min or incubated for 45 min in the presence of 15 μg/ml BFA (Sigma-Aldrich). For midbody isolation, cells

were synchronized at prometaphase and spindles were prepared as described previously (Kuriyama et al., 1984).

Fluorescence microscopy

Cells grown on coverslips or in 35-mm glass bottom microwell dishes were washed in PBS, fixed/permeabilized on ice for 30 min in 2% PFA + 0.1% Triton X-100, washed four times in PBS, and blocked for 15 min with 1% BSA (Sigma-Aldrich). Fixed cells were incubated in a moist chamber with primary antibody dissolved in 1% BSA for 1 h, followed by four washes of 5–10 min each in PBS before incubation with the secondary antibody dissolved in 1% BSA for another hour. After four further washes in PBS, samples were either observed immediately in PBS or mounted onto slides with Moviol and sealed with nail polish. Stained cells were observed under a Radiance 2000 AGR-3 (Q) confocal (Bio-Rad Laboratories) attached to an inverted microscope (model Axiovert S100TV; Carl Zeiss MicroImaging, Inc.) using 60× or 100× oil immersion lenses, and images were processed using Metamorph 4.6r9.

Electron microscopy

A431 cells were cultured on thermanox coverslips (Agar Scientific) and, after annexin 11 depletion, were fixed, processed, and treated with tannic acid as described by Stinchcombe et al. (1995). Coverslips were mounted on Epon stubs, the Epon polymerized overnight at 60°C, and the coverslips removed by heating. 70-nm sections were cut en face and stained with lead citrate before examination in a JEOL 1010 electron microscope.

Video time-lapse microscopy

A431 cells were placed in a 37°C preheated microscope chamber with 5% CO_2 supply and observed using phase illumination on an inverted microscope (model Axiovert S100M; Carl Zeiss MicroImaging, Inc.) using a 40× oil immersion lens. Images were acquired with Openlab (Improvision) and analyzed using Metamorph 4.6r9 (Universal Imaging Corp.).

Immunoprecipitation, SDS-PAGE, and Western blotting

A431 cell monolayers were washed in PBS, resuspended in 500 μl lysis buffer (50 mM Tris-Cl, pH 7.4, 50 mM NaCl, 30 mM sodium pyrophosphate, 50 mM sodium fluoride, 100 μM sodium orthovanadate, 0.2 mM $CaCl_2$, 1% Triton X-100, 0.1% BSA, and 0.02% sodium azide) supplemented with 10 μl of protease inhibitor cocktail (Sigma-Aldrich) per 10^7 cells, and lysed by three rounds of sonication on ice. Lysates were precleared at 16,000 *g* for 30 min at 4°C, followed by incubation with 30 μl of 50% protein G–Sepharose 4 Fast Flow slurry (Amersham Biosciences) for 30 min, and then 5 min centrifugation at 16,000 *g* at 4°C. L-19 goat anti–human annexin 11 antibody (Santa Cruz Biotechnology, Inc.) was immobilized on protein G–Sepharose beads and added to the precleared lysates for 2 h at 4°C, centrifuged, and the supernatant discarded. Beads were washed four times in lysis buffer minus BSA and once in ice-cold PBS. After removal of the supernatant, the immunoprecipitates were resuspended in SDS-PAGE sample buffer, boiled for 5 min, and resolved by SDS-PAGE on discontinuous mini-gels. Proteins were electroblotted for 45 min at 400 mA onto Hybond-P PVDF Transfer Membrane (Amersham Biosciences).

Membranes were treated with blocking solution (10% skimmed milk or 10% BSA in PBS-Tween [PBS + 0.05% Tween 20]) for 40 min at RT and incubated for 16 h at 4°C with primary antibody in PBS-Tween. After three PBS-Tween washes, membranes were incubated with secondary antibody for 90 min, also in PBS-Tween (1/10,000 dilution). IgG-HRP conjugates were used as secondary antibodies. Blots were developed after three further PBS-Tween washes using the ECL Plus Western blotting detection system (Amersham Biosciences) and visualized in a Fujifilm Intelligent Dark Box II coupled to a LAS-1000 CCD camera.

Depletion of annexin 11 in HeLa and A431 cells by RNAi

Preparation of siRNA oligonucleotides was performed as follows. A search was performed for AA(N19)TT sequences with ~50% G/C-content in human annexin 11 cDNA. One such sequence was located at nt 727 in the coding sequence. Sense (5′-gACggCUUACggCAAggAUdTdT-3′) and antisense (5′-AUCCUUgCCgUAAgCCgUCdTdT-3′) siRNA oligonucleotides were purchased from Dharmacon Research, Inc. Oligonucleotides were diluted with 1 ml of RNase-free water to a concentration of 50 μM and annealed by combining 30 μl of each with 15 μl of 5× annealing buffer (Dharmacon Research, Inc.). The solution was incubated at 90°C for 1 min followed by 1 h at 37°C. The final concentration of the siRNA duplex was 20 μM.

Transfection of cells with siRNA was performed as follows. Cells were seeded on 24-well plates in normal medium without antibiotics and transfected at 30 to 40% confluency as follows. For each well, 3 μl Oligofectamine reagent (Invitrogen) was dissolved in 12 μl Opti-MEM I medium (Invitrogen), and 3–5 μl of siRNA duplex was added to 50 μl of Opti-MEM I medium. The solutions were incubated for 10 min at RT, combined, and mixed by inversion. The mixture was incubated for 25 min at RT, and 30–32 μl of Opti-MEM I medium was added to bring the final volume to 100 μl. The complexes were added to the cells for 1 to 3 d before analysis by FACS®, immunofluorescence, or Western blotting. In some experiments, to further increase the depletion of annexin 11, transfected cells were split after 3 d and retransfected as aforementioned.

Fluorescence-activated cell sorting

To determine the level of apoptosis caused by annexin 11 depletion, siRNA-treated cells were analyzed by FACS®. Cells were collected, washed in PBS, fixed for 30 min in 70% ethanol at −20°C, centrifuged at 560 *g* for 5 min at 4°C, washed in PBS, and resuspended in 100 μl of 1 mg/ml RNase I-A (Sigma-Aldrich) solution in PBS for 30 min. To stain the DNA, 150 μl of propidium iodide solution (50 μg/ml propidium iodide [Sigma-Aldrich], 0.1% sodium citrate, and 0.1% Triton X-100) was added to this preparation. Samples were processed using a FACscan™ flowcytometer (BD Biosciences), and the results were analyzed with WinMDI 2.8.

Online supplemental material

Two supplemental figures are available showing the localization of annexin 11 and the Golgi marker GM130 in A431 cells undergoing cytokinesis and the localization of MKLP1 and Aurora B in annexin 11–depleted A431 cells undergoing cytokinesis. Videos showing control and annexin 11–depleted cells failing to complete cytokinesis are available as supplements to Fig. 7. Note that in Video 2 the apoptosing cells detach from the plate after the final frame. Online supplemental material is available at http://www.jcb.org/cgi/content/full/jcb.200311054/DC1.

We thank Dr. Ryoko Kuriyama for providing antisera to CHO1, Dr. Karl Matter for antisera to α-tubulin, and Ms. Grazyna Galatowitz for FACS® technical assistance.

This work was supported by the Wellcome Trust, the Medical Research Council, and Fight for Sight.

Submitted: 11 November 2003
Accepted: 10 May 2004

References

Altan-Bonnet, N., R.D. Phair, R.S. Polishchuk, R. Weigert, and J. Lippincott-Schwartz. 2003. A role for Arf1 in mitotic Golgi disassembly, chromosome segregation, and cytokinesis. *Proc. Natl. Acad. Sci. USA.* 100:13314–13319.

Boman, A.L., J. Kuai, X. Zhu, J. Chen, R. Kuriyama, and R.A. Kahn. 1999. Arf proteins bind to mitotic kinesin-like protein 1 (MKLP1) in a GTP-dependent fashion. *Cell Motil. Cytoskeleton.* 44:119–132.

Calabretta, B., R. Battini, L. Kaczmarek, J.K. de Riel, and R. Baserga. 1986. Molecular cloning of the cDNA for a growth factor-inducible gene with strong homology to S-100, a calcium-binding protein. *J. Biol. Chem.* 261: 12628–12632.

Chen, M.C., Y. Zhou, and H.W. Detrich III. 2002. Zebrafish mitotic kinesin-like protein 1 (Mklp1) functions in embryonic cytokinesis. *Physiol. Genomics.* 8:51–66.

Emoto, K., and M. Umeda. 2000. An essential role for a membrane lipid in cytokinesis. Regulation of contractile ring disassembly by redistribution of phosphatidylethanolamine. *J. Cell Biol.* 149:1215–1224.

Farnaes, L., and H.J. Ditzel. 2003. Dissecting the cellular functions of annexin XI using recombinant human annexin XI-specific autoantibodies cloned by phage display. *J. Biol. Chem.* 278:33120–33126.

Fernandez, M.P., N.A. Jenkins, D.J. Gilbert, N.G. Copeland, and R.O. Morgan. 1996. Sequence and chromosomal localization of mouse annexin XI. *Genomics.* 37:366–374.

Gerke, V., and S.E. Moss. 2002. Annexins: from structure to function. *Physiol. Rev.* 82:331–371.

Gromley, A., A. Jurczyk, J. Sillibourne, E. Halilovic, M. Mogensen, I. Groisman, M. Blomberg, and S. Doxsey. 2003. A novel human protein of the maternal centriole is required for the final stages of cytokinesis and entry into S phase. *J. Cell Biol.* 161:535–545.

Hawkins, T.E., J. Roes, D. Rees, J. Monkhouse, and S.E. Moss. 1999. Immuno-

logical development and cardiovascular function are normal in annexin VI null mutant mice. *Mol. Cell. Biol.* 19:8028–8032.

Hill, E., M. Clarke, and F.A. Barr. 2000. The Rab6-binding kinesin, Rab6-KIFL, is required for cytokinesis. *EMBO J.* 19:5711–5719.

Kuriyama, R., G. Keryer, and G.G. Borisy. 1984. The mitotic spindle of Chinese hamster ovary cells isolated in taxol-containing medium. *J. Cell Sci.* 66: 265–275.

Kuriyama, R., S. Dragas-Granoic, T. Maekawa, A. Vassilev, A. Khodjakov, and H. Kobayashi. 1994. Heterogeneity and microtubule interaction of the CHO1 antigen, a mitosis-specific kinesin-like protein. Analysis of subdomains expressed in insect sf9 cells. *J. Cell Sci.* 107:3485–3499.

Kuriyama, R., C. Gustus, Y. Terada, Y. Uetake, and J. Matuliene. 2002. CHO1, a mammalian kinesin-like protein, interacts with F-actin and is involved in the terminal phase of cytokinesis. *J. Cell Biol.* 156:783–790.

Lecuit, T., and E. Wieschaus. 2000. Polarized insertion of new membrane from a cytoplasmic reservoir during cleavage of the *Drosophila* embryo. *J. Cell Biol.* 150:849–860.

Litvak, V., D. Tian, S. Carmon, and S. Lev. 2002. Nir2, a human homolog of *Drosophila melanogaster* retinal degeneration B protein, is essential for cytokinesis. *Mol. Cell. Biol.* 22:5064–5075.

Matuliene, J., and R. Kuriyama. 2002. Kinesin-like protein CHO1 is required for the formation of midbody matrix and the completion of cytokinesis in mammalian cells. *Mol. Biol. Cell.* 13:1832–1845.

Mizutani, A., N. Usuda, H. Tokumitsu, H. Minami, K. Yasui, R. Kobayashi, and H. Hidaka. 1992. CAP-50, a newly identified annexin, localizes in nuclei of cultured fibroblast 3Y1 cells. *J. Biol. Chem.* 267:13498–13504.

Mizutani, A., N. Watanabe, T. Kitao, H. Tokumitsu, and H. Hidaka. 1995. The long amino-terminal tail domain of annexin XI is necessary for its nuclear localization. *Arch. Biochem. Biophys.* 318:157–165.

Morgan, R.O., D.W. Bell, J.R. Testa, and M.P. Fernandez. 1998. Genomic locations of ANX11 and ANX13 and the evolutionary genetics of human annexins. *Genomics.* 48:100–110.

Piel, M., J. Nordberg, U. Euteneuer, and M. Bornens. 2001. Centrosome-dependent exit of cytokinesis in animal cells. *Science.* 291:1550–1553.

Satoh, H., H. Shibata, Y. Nakano, Y. Kitaura, and M. Maki. 2002. ALG-2 interacts with the amino-terminal domain of annexin XI in a Ca^{2+}-dependent manner. *Biochem. Biophys. Res. Commun.* 291:1166–1172.

Scovassi, A.I., and G.G. Poirier. 1999. Poly(ADP-ribosylation) and apoptosis. *Mol. Cell. Biochem.* 199:125–137.

Sellitto, C., and R. Kuriyama. 1988. Distribution of a matrix component of the midbody during the cell cycle in Chinese hamster ovary cells. *J. Cell Biol.* 106:431–439.

Sisson, J.C., C. Field, R. Ventura, A. Royou, and W. Sullivan. 2000. Lava lamp, a novel peripheral golgi protein, is required for *Drosophila melanogaster* cellularization. *J. Cell Biol.* 151:905–918.

Skop, A.R., D. Bergmann, W.A. Mohler, and J.G. White. 2001. Completion of cytokinesis in *C. elegans* requires a brefeldin A-sensitive membrane accumulation at the cleavage furrow apex. *Curr. Biol.* 11:735–746.

Stinchcombe, J., D. Cutler, and C.R. Hopkins. 1995. Anterograde and retrograde traffic between the endoplasmic reticulum and the Golgi complex. *J. Cell Biol.* 131:1387–1401.

Straight, A.F., and C.M. Field. 2000. Microtubules, membranes and cytokinesis. *Curr. Biol.* 10:R760–R770.

Terada, Y., M. Tatsuka, F. Suzuki, Y. Yasuda, S. Fujita, and M. Otsu. 1998. AIM-1: a mammalian midbody-associated protein required for cytokinesis. *EMBO J.* 17:667–676.

Tokumitsu, H., A. Mizutani, H. Minami, R. Kobayashi, and H. Hidaka. 1992. A calcyclin-associated protein is a newly identified member of the Ca^{2+}/phospholipid-binding proteins, annexin family. *J. Biol. Chem.* 267:8919–8924.

Tokumitsu, H., A. Mizutani, and H. Hidaka. 1993. Calcyclin-binding site located on the NH_2-terminal domain of rabbit CAP-50 (annexin XI): functional expression of CAP-50 in *Escherichia coli*. *Arch. Biochem. Biophys.* 303:302–306.

Tomas, A., and S.E. Moss. 2003. Calcium- and cell cycle-dependent association of annexin 11 with the nuclear envelope. *J. Biol. Chem.* 278:20210–20216.

Towle, C.A., and B.V. Treadwell. 1992. Identification of a novel mammalian annexin. cDNA cloning, sequence analysis, and ubiquitous expression of the annexin XI gene. *J. Biol. Chem.* 267:5416–5423.

Xu, H., J.A. Brill, J. Hsien, R. McBride, G.L. Boulianne, and W.S. Trimble. 2002. Syntaxin 5 is required for cytokinesis and spermatid differentiation in *Drosophila*. *Dev. Biol.* 251:294–306.

Yasui, Y., M. Amano, K. Nagata, N. Inagaki, H. Nakamura, H. Saya, K. Kaibuchi, and M. Inagaki. 1998. Roles of Rho-associated kinase in cytokinesis; mutations in Rho-associated kinase phosphorylation sites impair cytokinetic segregation of glial filaments. *J. Cell Biol.* 143:1249–1258.